MHD FLOW AND HEAT TRANSFER OF TWO IMMISCIBLE FLUIDS BETWEEN MOVING PLATES

Stamenković M. Živojin[1], Dragiša D. Nikodijević[1], Bratislav D. Blagojević[1], Slobodan R. Savić[2]

[1] *University of Niš, Faculty of Mechanical Engineering, Serbia*
[2] *University of Kragujevac, Faculty of Mechanical Engineering, Serbia,*
E-mail: zikas@masfak.ni.ac.rs

Received January 2010, Accepted September 2010
No. 10-CSME-01, E.I.C. Accession 3164

ABSTRACT

The magnetohydrodynamic (MHD) flow of two immiscible and electrically conducting fluids between isothermal, insulated moving plates in the presence of an applied electric and inclined magnetic field has been investigated in the paper. The partial differential equations governing the flow and heat transfer are solved analytically with appropriate boundary conditions for each fluid and these solutions have been matched at the interface. The numerical results for various values of the Hartmann number, the angle of magnetic field inclination, load parameter and the ratio of electrical and thermal conductivities have been presented graphically. It was found that decrease of magnetic field inclination angle flattens out the velocity and temperature profiles. With the increase of the Hartmann number velocity gradients near the plate's increases, temperature in the middle of the channel decreases and near the plate's increases. Induced magnetic field is evidently suppressed with an increase of the Hartman number. The effect of changes of the load factor is to aid or oppose the flow as compared to the short-circuited case.

Keywords: MHD, immiscible fluids, moving plates, heat transfer, induced magnetic field.

DÉBIT MHD ET TRANSFERT DE CHALEUR DE DEUX FLUIDES IMMISCIBLES ENTRE DES PLATEAUX MOBILES

RÉSUMÉ

La recherche présente une étude sur le débit magnétohydrodynamique (MHD) de deux fluides immiscibles, conducteur du courant électrique entre des plateaux mobiles isolés, isothermes, en présence d'un champ magnétique appliqué incliné. Les équations différentielles partielles régissant le débit et le transfert de chaleur sont résolues de façon analytique avec des conditions limites appropriées pour chaque fluide, ses solutions appliquées ayant été appariées à l'interface. Les résultats numériques pour les différentes valeurs du nombre de Hartmann, l'angle d'inclinaison du champ magnétique, les paramètres de charge et le ratio des conductivités électriques et thermiques sont représentés dans un graphique. On a constaté que la réduction de l'angle d'inclinaison du champ magnétique stabilise les profils de la célérité et de la température. Avec l'augmentation du nombre de Hartmann, les gradients de célérité augmentent près des plateaux, pendant que la température au centre du canal diminue, et augmente près des plateaux. Par le fait même, l'aimantation induite est supprimée avec l'augmentation du nombre de Hartmann. Les changements du facteur de charge a pour effet d'aider ou de contrer le débit, contrairement à un court-circuit.

Mots-clés : MHD; fluides immiscibles; plateaux mobiles; transfert de chaleur; champ magnétique induit.

Nomenclature (Optional Section)

B	magnetic field vector (T)
B_0	strength of applied magnetic field (T)
B_x	strength of induced magnetic field (T)
b_i	dimensionless ratio of magnetic fields
c_p	specific heat capacity (J/kgK)
C_i	constants
D_{ij}	constants
E	electric field vector (V/m)
F_i	constants
Ha_i	Hartmann number in region i
h	half channel height (m)
J	current density vector (A/m^2)
K	load factor
k_i	thermal conductivity of fluid in region i (W/Km)
L	constant
M_i	constants
p	pressure (Pa)
Q_{ij}	constants
Rm_i	magnetic Reynolds number in region i
S	constant
T	temperature (K)
t	time (s)
U_0	absolute velocity of plates (m/s)
u_i	fluid velocity in x-direction in region i (m/s)
v	velocity vector (m/s)
x	longitudinal coordinate (m)
y	transversal coordinate (m)
W	constant

Greek symbols

α	viscosities ratio of fluids
δ	ratio of magnetic permeability's
γ	ratio of electrical conductivities
Φ	dissipative function
λ	cosine of inclination angle θ
μ_i	dynamic viscosity of fluid in region i (kg/ms)
μ_{ei}	magnetic permeability of fluid in region i (H/m)
ν_i	kinematic viscosity of fluid in region i (m^2/s)
θ	applied magnetic filed inclination angle (^{o})
Θ_i	dimensionless temperature in region i
ρ_i	density of fluid in region i (kg/m^3)
σ_i	electrical conductivity of fluid in region i (S/m)
ξ	ratio of thermal conductivities
$\Im_i$	constants

Subscripts

1	fluid in region 1
2	fluid in region 2
w	plate
$*$	dimensionless quantities

1 INTRODUCTION

The flow and heat transfer of electrically conducting fluids in channels and circular pipes under the effect of a transverse magnetic field occurs in magnetohydrodynamic (MHD) generators, pumps, accelerators and flowmeters and have applications in nuclear reactors, filtration, geothermal systems and others.

The interest in the outer magnetic field effect on heat-physical processes appeared seventy years ago. Research in magnetohydrodynamics grew rapidly during the late 1950s as a result of extensive studies of ionized gases for a number of applications. Blum et al. [1] carried out one of the first works in the field of heat and mass transfer in the presence of a magnetic field. The

increasing interest in the study of MHD phenomena is also related to the development of fusion reactors where plasma is confined by a strong magnetic field [2]. Morley et al. [3] studied MHD effects in the so called blanket. Blanket is located between the plasma and the magnetic field coils, absorbs neutrons transforming their energy into heat, which is then carried away by a suitable coolant and it prevents neutrons from reaching the magnets avoiding in this way radiation damages. Many exciting innovations were put forth in the areas of MHD propulsion [4], remote energy deposition for drag reduction [5], plasma actuators, radiation driven hypersonic wind tunnel, MHD control of flow and heat transfer in the boundary layer [6,7,8,9], enhanced plasma ignition [10] and combustion stability. Extensive research however has revealed that additional and refined fidelity of physics in modeling and analyzing the interdisciplinary endeavor are required to reach a conclusive assessment. In order to ensure a successful and effective use of electromagnetic phenomena in industrial processes and technical systems, a very good understanding of the effects of the application of a magnetic field on the flow of electrically conducting fluids in channels and various geometric elements is required. From this lesson learned; most recent research activities tend to refocus to basic and simpler fluid dynamic-electromagnetic interaction phenomena.

All the mentioned studies pertain to a single-fluid model. Most of the problems relating to the petroleum industry, geophysics, plasma physics, magneto-fluid dynamics, etc., involve multi-fluid flow situations. The problem concerning the flow of immiscible fluids has a definite role in chemical engineering and in medicine [11]. There have been some experimental and analytical studies on hydrodynamic aspects of the two-fluid flow reported in the literature. Bird et al. [12] obtained an exact solution for the laminar flow of two immiscible fluids between parallel plates. Bhattacharya [13] investigated the flow of two immiscible fluids between two rigid parallel plates with a time-dependent pressure gradient. Later, Mitra [14] analyzed the unsteady flow of two electrically conducting fluids between two rigid parallel plates. The physical situation discussed by Mitra is one possible case. Another physical phenomenon is the case in which the two immiscible conducting fluids flow past permeable beds. Chamkha [15] reported analytical solutions for flow of two-immiscible fluids in porous and non-porous parallel-plate channels. The findings of a study of this physical phenomenon have a definite bearing on petroleum and chemical technologies and on biomechanics.

These examples show the importance of knowledge of the laws governing immiscible multi-phase flows for proper understanding of the processes involved. In modeling such problems, the presence of a second immiscible fluid phase adds a number of complexities as to the nature of interacting transport phenomena and interface conditions between the phases. There has been some theoretical and experimental work on stratified laminar flow of two immiscible fluids in a horizontal pipe [16–19]. Loharsbi et al. [20] studied two-phase MHD flow and heat transfer in a parallel plate channel with one of the fluids being electrically conducting. Following the ideas of Alireaz et al. [16], Malashetty et al. [21, 22] have studied the two-fluid MHD flow and heat transfer in an inclined channel, and flow in an inclined channel containing porous and fluid layer. Umavathi et al. [23, 24] have presented analytical solutions of an oscillatory Hartmann two-fluid flow and heat transfer in a horizontal channel and an unsteady two-fluid flow and heat transfer in a horizontal channel. Recently, Malashetty et al. [25] have analyzed the problem of magnetoconvection of two-immiscible fluids in vertical enclosure.

Keeping in view the wide area of practical importance of multi-fluid flows as mentioned above, the objective of the present study is to investigate the MHD flow and heat transfer of two immiscible fluids between moving plates in the presence of applied electric and inclined magnetic field.

2 MATHEMATICAL MODEL

As mentioned in the introduction, the problem of the MHD two-fluid flow between parallel moving plates has been considered in this paper. MHD channel flow analysis is usually performed assuming the fluid constant electrical conductivity and treating the problem as a mono-dimensional one: with these two main assumptions the governing equations are considerably simplified and they can be solved analytically without causing significant errors for simple channel geometry [26]. In this paper, usual flow analysis has been extended considering induced magnetic filed in order to analyze the magnetohydrodynamic interaction and in energy equation besides the viscous heating, Joule heating is taken into account.

The fluids in the two regions have been assumed immiscible and incompressible and the flow has been steady, one-dimensional and fully developed. Furthermore, the two fluids have different kinematic viscosities v_1 and v_2 and densities ρ_1 and ρ_2. The physical model shown in Fig. 1, consists of two infinite parallel plates extending in the x and z-direction. The upper plate moves with constant velocity U_0 in positive longitudinal direction, while lower plates moves with same velocity but in opposite direction. The region 1: $0 \le y \le h$ has been occupied by a fluid of viscosity μ_1, electrical conductivity σ_1, and thermal conductivity k_1, and the region 2: $-h \le y \le 0$ has been filled by a layer of different fluid of viscosity μ_2, thermal conductivity k_2 and electrical conductivity σ_2.

A uniform magnetic field of the strength B_0 has been applied in the direction making an angle θ to the y axis and due the fluid motion magnetic field of the strength B_x has been induced along the lines of motion.

The fluid velocity $\vec{\mathbf{v}}$ and the magnetic field distributions are:

$$\vec{\mathbf{v}} = (u(y),0,0); \tag{1}$$

$$\vec{\mathbf{B}} = \left(B_x(y) + B_0\sqrt{1-\lambda^2}, B_0\lambda, 0\right); \tag{2}$$

where $\vec{\mathbf{B}}$ is magnetic field vector and $\lambda = \cos\theta$.

The upper and lower plate have been kept at the two constant temperatures T_{w1} and T_{w2}, respectively, and the plates are electrically insulated.

The described MHD two-fluid flow problem is mathematically presented with a continuity equation:

$$\nabla\vec{\mathbf{v}} = 0; \tag{3}$$

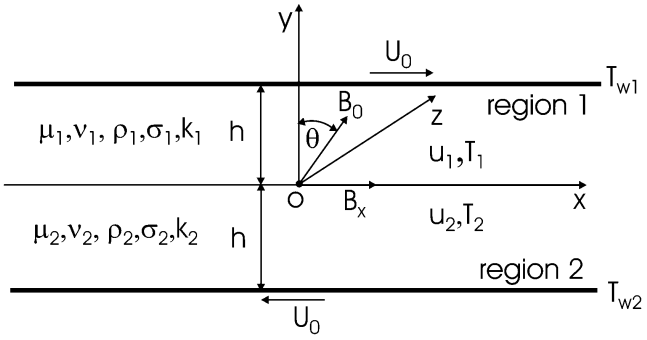

Fig. 1. Physical model and coordinate system.

momentum equation:

$$\rho\left\{\frac{\partial\vec{\mathbf{v}}}{\partial t}+(\vec{\mathbf{v}}\nabla)\vec{\mathbf{v}}\right\}=-\nabla p+\mu\nabla^2\vec{\mathbf{v}}+\vec{\mathbf{J}}\times\vec{\mathbf{B}};\tag{4}$$

magnetic induction equation:

$$\frac{\partial\vec{\mathbf{B}}}{\partial t}-\nabla\times\left(\vec{\mathbf{v}}\times\vec{\mathbf{B}}\right)-\frac{1}{\sigma\mu_e}\nabla^2\vec{\mathbf{B}}=0;\tag{5}$$

and an energy equation:

$$\rho c_p\left(\frac{\partial T}{\partial t}+\vec{\mathbf{v}}\nabla T\right)=k\nabla^2T+\mu\Phi+\frac{\vec{\mathbf{J}}^2}{\sigma};\tag{6}$$

where:

$$\begin{aligned}\Phi=2&\left[\left(\frac{\partial u}{\partial x}\right)^2+\left(\frac{\partial v}{\partial y}\right)^2+\left(\frac{\partial w}{\partial z}\right)^2\right]+\\&+\left(\frac{\partial v}{\partial x}+\frac{\partial u}{\partial y}\right)^2+\left(\frac{\partial w}{\partial y}+\frac{\partial v}{\partial z}\right)^2+\left(\frac{\partial u}{\partial z}+\frac{\partial w}{\partial x}\right)^2-\frac{2}{3}(\nabla\vec{\mathbf{v}})^2.\end{aligned}\tag{7}$$

In previous general equations and in following boundary conditions, applicable for both fluid regions, used symbols are common for the theory of MHD flows. The third term on the right hand side of Eq. (4) is the magnetic body force and $\vec{\mathbf{J}}$ is the current density vector defined by:

$$\vec{\mathbf{J}}=\sigma\left(\vec{\mathbf{E}}+\vec{\mathbf{v}}\times\vec{\mathbf{B}}\right);\tag{8}$$

where $\vec{\mathbf{E}}=(0,0,E_z)$ is the vector of the applied electric field.

Using the velocity, magnetic and electric field distribution as stated above, the Eq. (4) to Eq. (6) are as follows:

$$\frac{1}{\rho}P+\nu\frac{d^2u}{dy^2}-\frac{\sigma}{\rho}B_0\lambda(E_z+uB_0\lambda)=0;\tag{9}$$

$$B_0\lambda\frac{du}{dy}+\frac{1}{\sigma\mu_e}\frac{d^2B_x}{dy^2}=0;\tag{10}$$

$$\rho c_pu\frac{\partial T}{\partial x}=k\frac{\partial^2T}{\partial y^2}+\mu\left(\frac{\partial u}{\partial y}\right)^2+\sigma(E_z+uB_0\lambda)^2;\tag{11}$$

where:

$$P = -\frac{\partial p}{\partial x}. \tag{12}$$

The flow and thermal boundary conditions have been unchanged by the addition of electromagnetic fields. The no slip conditions require that the fluid velocities are equal to the plate's velocities and boundary conditions on temperature are isothermal conditions. In addition, the fluid velocity, induced magnetic field, sheer stress and heat flux must be continuous across the interface $y = 0$. Equations which represent these conditions for fluids in regions 1 and 2 are:

$$u_1(h) = U_0,\ u_2(-h) = -U_0; \tag{13}$$

$$u_1(0) = u_2(0); \tag{14}$$

$$\mu_1 \frac{du_1}{dy} = \mu_2 \frac{du_2}{dy},\ y = 0; \tag{15}$$

$$B_{x1}(h) = 0,\ B_{x2}(-h) = 0; \tag{16}$$

$$B_{x1}(0) = B_{x2}(0); \tag{17}$$

$$\frac{1}{\mu_{e1}\sigma_1}\frac{dB_{x1}}{dy} = \frac{1}{\mu_{e2}\sigma_2}\frac{dB_{x2}}{dy} \text{ for } y = 0; \tag{18}$$

$$T_1(h) = T_{w1},\ T_2(-h) = T_{w2}; \tag{19}$$

$$T_1(0) = T_2(0); \tag{20}$$

$$k_1 \frac{dT_1}{dy} = k_2 \frac{dT_2}{dy};\ y = 0. \tag{21}$$

3 VELOCITY AND MAGNETIC FIELD DISTRIBUTION

The governing equation for the velocity u_i in regions 1 and 2 can be written as:

$$\frac{1}{\rho_i}P + v_i \frac{d^2 u_i}{dy^2} - \frac{\sigma_i}{\rho_i} B_0 \lambda (E_z + u_i B_0 \lambda) = 0; \tag{22}$$

where suffix i ($i=1,2$) represent the values for the regions 1 and 2 respectively. The equation for the magnetic field induction in the regions 1 and 2 can be written as:

$$B_0\lambda\frac{du_i}{dy}+\frac{1}{\sigma_i\mu_{ei}}\frac{d^2B_{xi}}{dy^2}=0. \tag{23}$$

It is convenient to transform the Eqs. (22) and (23) to a dimensionless form:

$$\frac{d^2u_i^*}{dy^{*2}}-Ha_i^2\left(K+u_i^*\lambda\right)\lambda+G_i=0; \tag{24}$$

$$\frac{d^2b_i}{dy^{*2}}+\lambda Rm_i\frac{du_i^*}{dy^*}=0; \tag{25}$$

where following dimensionless quantities have been used:

$$u_i^*=\frac{u_i}{U_0},\ y^*=\frac{y}{h}; \tag{26}$$

$$\alpha=\frac{\mu_1}{\mu_2},\ \gamma=\frac{\sigma_1}{\sigma_2},\ \delta=\frac{\mu_{e1}}{\mu_{e2}}; \tag{27}$$

$$G_i=\frac{P}{(\mu_iU_0/h^2)},\ b_i=\frac{B_{xi}}{B_0}; \tag{28}$$

$$K=\frac{E_z}{U_0B_0}-\text{load parameter}; \tag{29}$$

$$Ha_i=B_0h\sqrt{\frac{\sigma_i}{\mu_i}}-\text{ Hartmann number}; \tag{30}$$

$$Rm_i=U_0h\sigma_i\mu_{ei}-\text{magnetic Reynolds number}. \tag{31}$$

The dimensionless form of the boundary and interface conditions (13) to (18) becomes:

$$u_1^*(1)=1,\ u_2^*(-1)=-1; \tag{32}$$

$$u_1^*(0)=u_2^*(0); \tag{33}$$

$$\frac{du_1^*}{dy^*} = \frac{1}{\alpha}\frac{du_2^*}{dy^*} \text{ for } y^* = 0; \tag{34}$$

$$b_1(1) = 0,\ b_2(-1) = 0; \tag{35}$$

$$b_1(0) = b_2(0); \tag{36}$$

$$\frac{db_1}{dy^*} = \delta\gamma\frac{db_2}{dy^*} \text{ for } y^* = 0. \tag{37}$$

The solutions of Eqs. (24) and (25) with boundary and interface conditions have the following forms:

$$u_i^*(y^*) = D_{1i}\cosh(\lambda Ha_i y^*) + D_{2i}\sinh(\lambda Ha_i y^*) + F_i; \tag{38}$$

$$b_i(y^*) = -\frac{Rm_i}{Ha_i}[D_{1i}\sinh(\lambda Ha_i y^*) + D_{2i}\cosh(\lambda Ha_i y^*)] + Q_{1i}y^* + Q_{2i}; \tag{39}$$

where:

$$F_i = \frac{G_i}{\lambda^2 Ha_i^2} - \frac{K}{\lambda}; \tag{40}$$

$$D_{11} = \frac{(1-F_1)H\sinh(\lambda Ha_2)}{W} - \frac{L\sinh(\lambda Ha_1)}{W}; \tag{41}$$

$$L = 1 + F_2 + S\cosh(\lambda Ha_2); \tag{42}$$

$$W = H\cosh(\lambda Ha_1)\sinh(\lambda Ha_2) + \cosh(\lambda Ha_2)\sinh(\lambda Ha_1); \tag{43}$$

$$H = \alpha\frac{Ha_1}{Ha_2}; \tag{44}$$

$$S = \frac{1}{\lambda^2}\left(\frac{G_1}{Ha_1^2} - \frac{G_2}{Ha_2^2}\right); \tag{45}$$

$$D_{21} = \frac{(1-F_1)\cosh(\lambda Ha_2)}{W} + \frac{L\cosh(\lambda Ha_1)}{W}; \tag{46}$$

$$D_{12} = S + D_{11}; \tag{47}$$

$$D_{22} = HD_{21}; \tag{48}$$

$$Q_{11} = Rm_1\lambda D_{11} + \delta\gamma(Q_{12} - \lambda Rm_2 D_{12}); \tag{49}$$

$$Q_{21} = \frac{Rm_1}{Ha_1}[D_{11}\sinh(\lambda Ha_1) + D_{21}\cosh(\lambda Ha_1)] - Q_{11}; \tag{50}$$

$$Q_{12} = \frac{M_1 + M_2}{1+\delta\gamma}; \tag{51}$$

$$M_1 = \frac{Rm_1}{Ha_1}\{D_{11}[\sinh(\lambda Ha_1) - \lambda Ha_1] + D_{21}[\cosh(\lambda Ha_1) - 1]\}; \tag{52}$$

$$M_2 = \frac{Rm_2}{Ha_2}\{D_{12}[\sinh(\lambda Ha_2) + \lambda\delta\gamma Ha_2] + D_{22}[1 - \cosh(\lambda Ha_2)]\}; \tag{53}$$

$$Q_{22} = \frac{Rm_2}{Ha_2}[D_{22}\cosh(\lambda Ha_2) - D_{12}\sinh(\lambda Ha_2)] + Q_{12}. \tag{54}$$

4 TEMPERATURE DISTRIBUTION

Once the velocity distributions were known, the temperature distributions for the two regions have been determined by solving the energy equation subject to the appropriate boundary and interface conditions (19)–(21). In the present problem, it has been assumed that the two plates have been maintained at constant temperatures. The term involving $\partial T/\partial x = 0$ in the energy Eq. (11) drops out for such a condition. The governing equation for the temperatures T_1 and T_2 in regions 1 and 2 is then given by:

$$k_i\frac{d^2T_i}{dy^2} + \mu_i\left(\frac{du_i}{dy}\right)^2 + \sigma_i(E_z + u_iB_0\lambda)^2 = 0. \tag{55}$$

In order to obtain dimensionless form of the previous equation, the following transformations

have been used beside the already introduced (26) to (31):

$$\Theta_i = \frac{T_i - T_{wi}}{U_0^2 \frac{\mu_i}{k_i}},\ \xi = \frac{k_1}{k_2}. \tag{56}$$

With the above dimensionless quantities Eq. (55) for regions 1 and 2 becomes:

$$\frac{d^2\Theta_i}{dy^{*2}} + \left(\frac{du_i^*}{dy^*}\right)^2 + Ha_i^2\left(K + u_i^*\lambda\right)^2 = 0. \tag{57}$$

In the non-dimensional form, the boundary conditions for temperature and heat flux at the interface $y = 0$ becomes:

$$\Theta_1(1) = 0,\ \Theta_2(-1) = 0; \tag{58}$$

$$\Theta_1(0) = \frac{\xi}{\alpha}\Theta_2(0) + S^*; \tag{59}$$

$$S^* = \frac{1}{U_0^2}\frac{k_1}{\mu_1}(T_{w2} - T_{w1}); \tag{60}$$

$$\frac{d\Theta_1}{dy^*} = \frac{1}{\alpha}\frac{d\Theta_2}{dy^*},\ y^* = 0. \tag{61}$$

The solution of Eq. (57) with boundary and interface conditions has the following form:

$$\begin{aligned}\Theta_i(y^*) = -\frac{1}{4\lambda}\{&\lambda\left(D_{1i}^2 + D_{2i}^2\right)\cosh(2\lambda Ha_i y^*) + 8D_{2i}C_i\sinh(\lambda Ha_i y^*) + \\ &+ 2D_{1i}D_{2i}\lambda\sinh(2\lambda Ha_i y^*) + 8D_{1i}C_i\cosh(\lambda Ha_i y^*) \\ &- 2\lambda\left(2D_{3i} + 2D_{4i}y^* - {Ha_i}^2 C_i^2 y^{*2}\right)\};\end{aligned} \tag{62}$$

where:

$$C_i = K + \lambda F_i = \frac{G_i}{\lambda Ha_i^2},\ i = 1,2; \tag{63}$$

$$D_{31} = \frac{\xi}{\alpha}D_{42} + \frac{\xi}{\alpha}\Im_2 + \Im_3; \tag{64}$$

$$D_{41} = \frac{1}{\alpha} D_{42} + \Im_4; \tag{65}$$

$$D_{32} = D_{42} + \Im_2; \tag{66}$$

$$D_{42} = \frac{\alpha}{\xi + 1} \left(\Im_1 - \frac{\xi}{\alpha} \Im_2 - \Im_3 - \Im_4 \right); \tag{67}$$

$$\begin{aligned} \Im_1 = \frac{1}{4\lambda} \{ & \lambda \left(D_{11}^2 + D_{21}^2 \right) \cosh(2\lambda Ha_1) + 8 D_{21} C_1 \sinh(\lambda Ha_1) + \\ & + 2 D_{11} D_{21} \lambda \sinh(2\lambda Ha_1) + 8 D_{11} C_1 \cosh(\lambda Ha_1) + 2\lambda {Ha_1}^2 C_1^2 \}; \end{aligned} \tag{68}$$

$$\begin{aligned} \Im_2 = \frac{1}{4\lambda} \{ & \lambda \left(D_{12}^2 + D_{22}^2 \right) \cosh(2\lambda Ha_2) - 8 D_{22} C_2 \sinh(\lambda Ha_2) - \\ & - 2 D_{12} D_{22} \lambda \sinh(2\lambda Ha_2) + 8 D_{12} C_2 \cosh(\lambda Ha_2) + 2\lambda {Ha_2}^2 C_2^2 \}; \end{aligned} \tag{69}$$

$$\Im_3 = \frac{1}{4} \left[D_{11}^2 + D_{21}^2 - \frac{\xi}{\alpha} \left(D_{12}^2 + D_{22}^2 \right) \right] + \frac{2}{\lambda} \left(D_{11} C_2 - \frac{\xi}{\alpha} D_{12} C_2 \right) + S^*; \tag{70}$$

$$\Im_4 = D_{21}(2C_1 + \lambda D_{11}) Ha_1 - \frac{1}{\alpha} D_{22}(2C_2 + \lambda D_{12}) Ha_2. \tag{71}$$

5 RESULTS AND DISCUSSION

In this section, flow and heat transfer results for steady MHD flow of two immiscible fluids between moving plates are presented and discussed for various values of selected parameters. Dimensionless velocity, temperature and magnetic field induction are presented graphically in Figs. 2 to 14 for the two fluids important for technical practice and the parameters α,ξ,γ,δ and S^* take the values of 0.66; 0.06; 0.025; 1 and 0 respectively.

The Figs. 2 to 4 show the effect of the magnetic field inclination angle on the distribution of velocity, temperature and the ratio of the applied and induced magnetic field.

Figure 2 shows the effect of the angle of inclination on velocity which predicts that the velocity increases as the inclination angle increases. These results are expected because the application of a transverse magnetic field normal to the flow direction has a tendency to create a drag-like Lorentz force which has a decreasing effect on the flow velocity.

In Fig. 3, the dimensionless temperature distribution as a function of y^*, for various values of applied magnetic field inclination angle, is shown. The Fig. 3 shows an dimensionless temperature jump at the interface, which results from choice of Θ_i (the thermodynamic

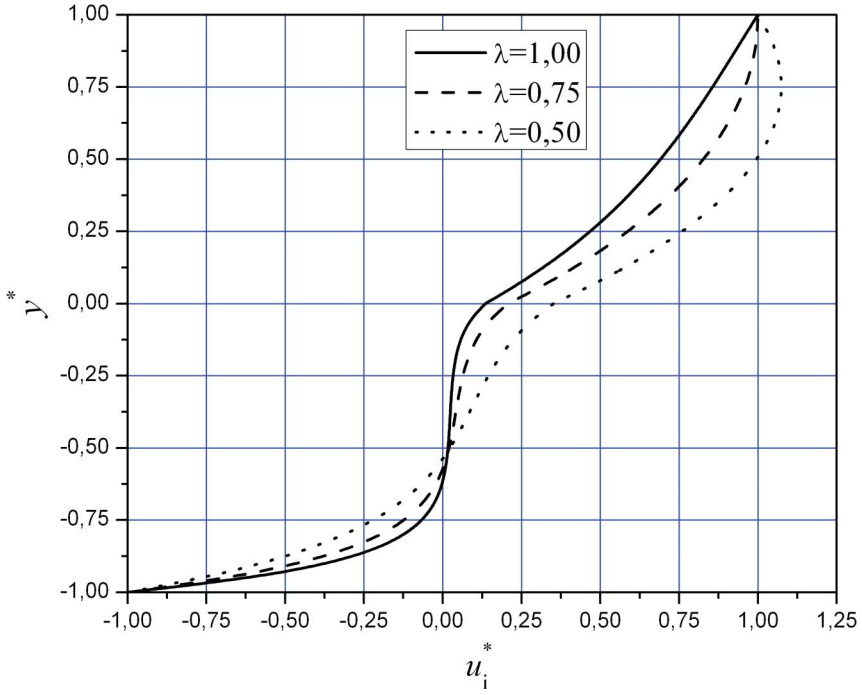

Fig. 2. Velocity profiles for different values of magnetic field inclination angle ($Ha_1 = 2$; $Ha_2 = 10$; $K = 0$; $\alpha = 0.66$; $\gamma = 0.025$; $\xi = 0.06$).

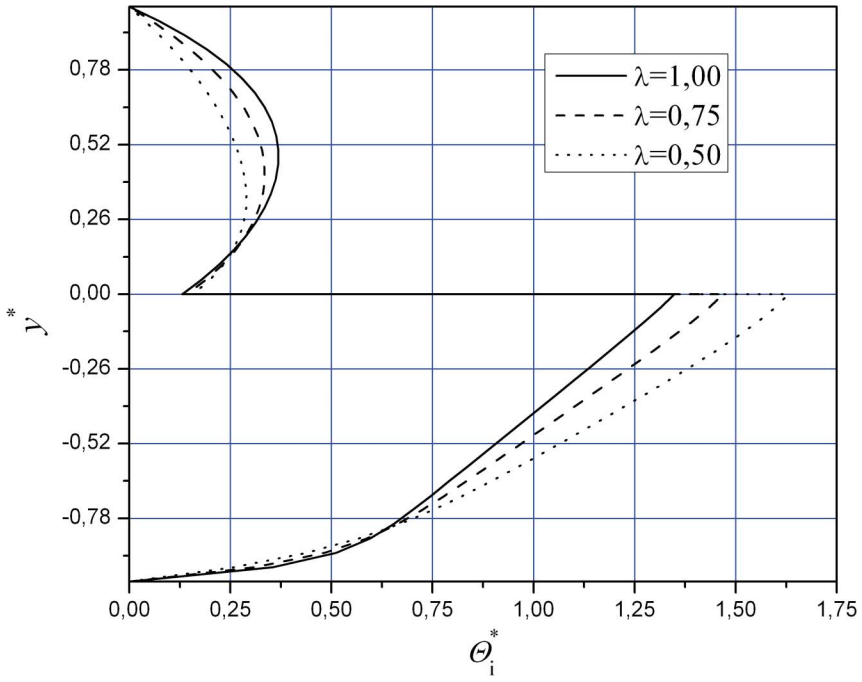

Fig. 3. Temperature profiles for different values of magnetic field inclination angle ($Ha_1 = 2$; $Ha_2 = 10$; $K = 0$; $\alpha = 0.66$; $\gamma = 0.025$; $\xi = 0.06$).

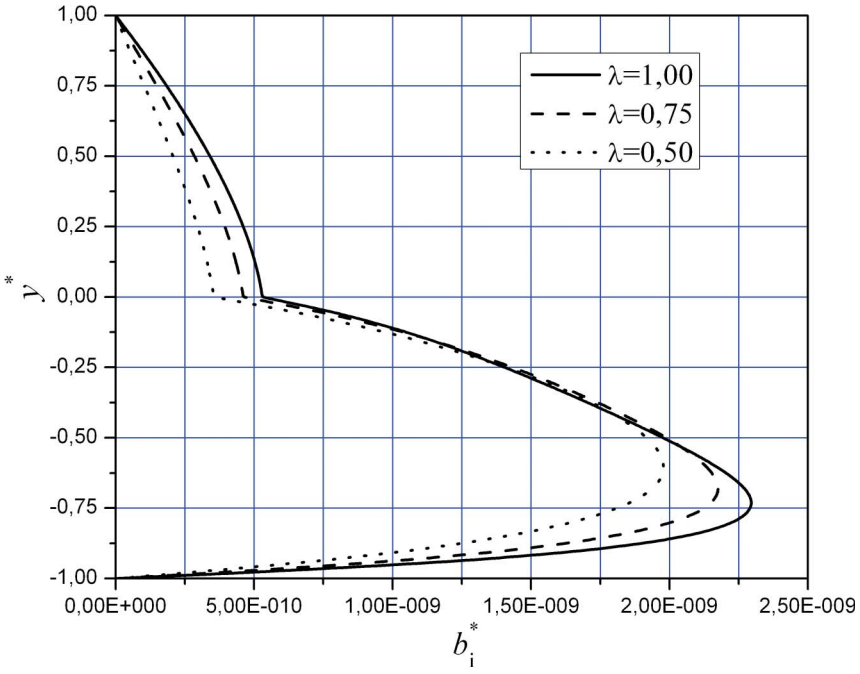

Fig. 4. Ratio of an induced and applied magnetic field for different values of λ ($Ha_1 = 2$; $Ha_2 = 10$; $K = 0$; $\alpha = 0.66$; $\gamma = 0.025$; $\xi = 0.06$).

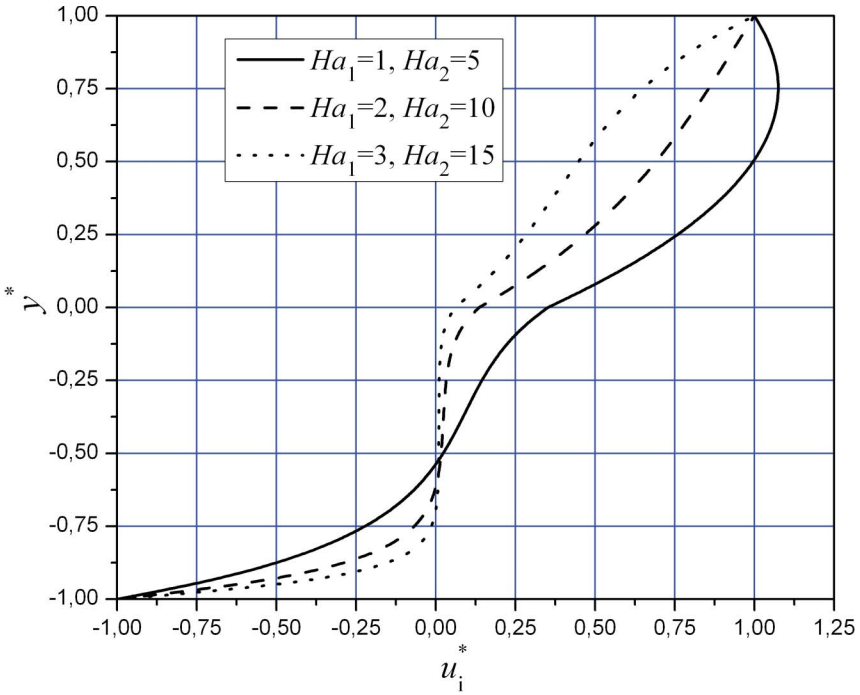

Fig. 5. Velocity profiles for different values of Hartmann numbers Ha_i ($K = 0$; $\alpha = 0.66$; $\lambda = 1$; $\gamma = 0.025$; $\xi = 0.06$).

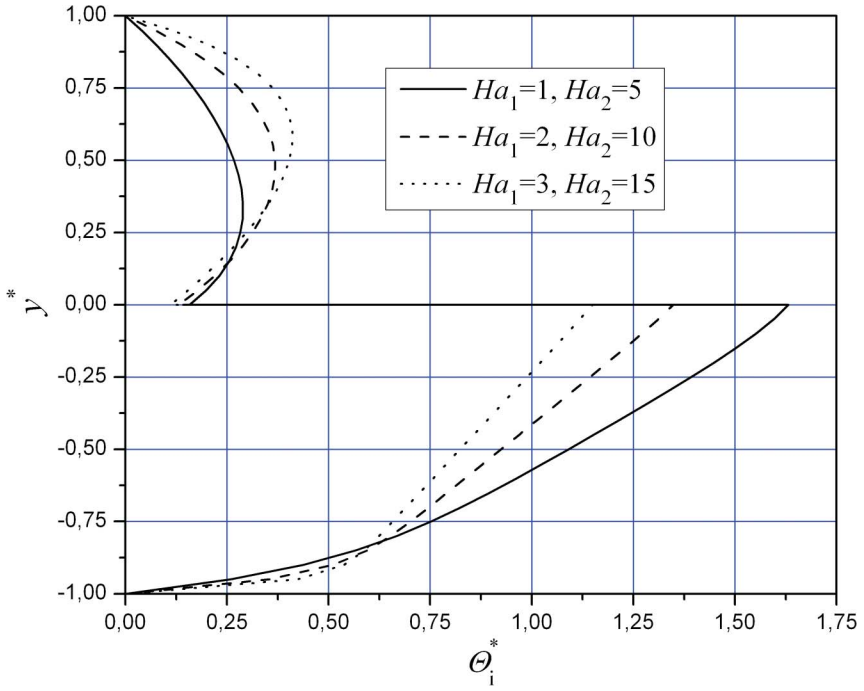

Fig. 6. Temperature profiles for different values of Hartmann numbers Ha_i ($K=0; \alpha=0.66; \lambda=1; \gamma=0.025; \xi=0.06$).

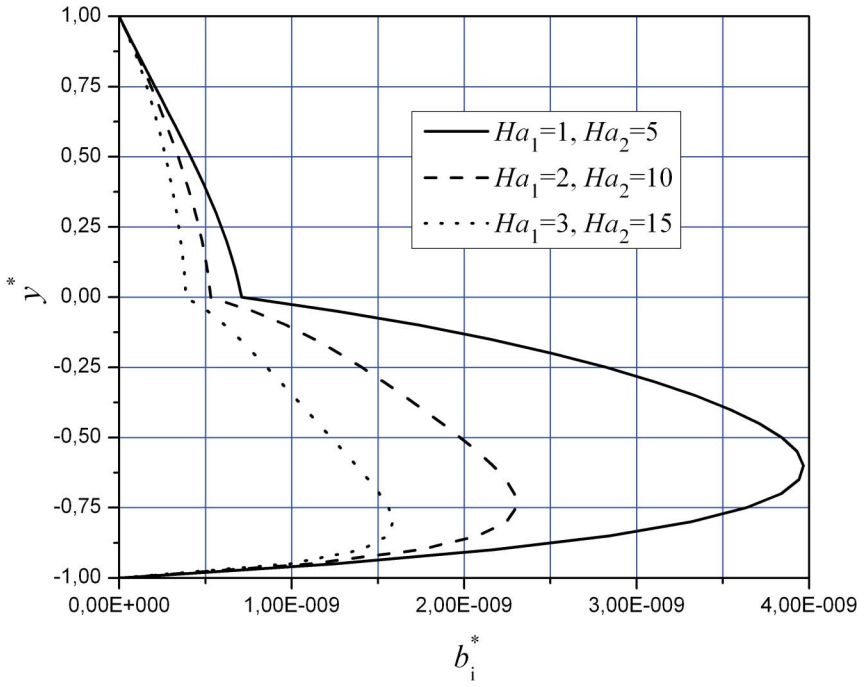

Fig. 7. Ratio of an induced and applied magnetic field for different values of Hartmann numbers Ha_i ($K=0; \alpha=0.66; \lambda=1; \gamma=0.025; \xi=0.06$).

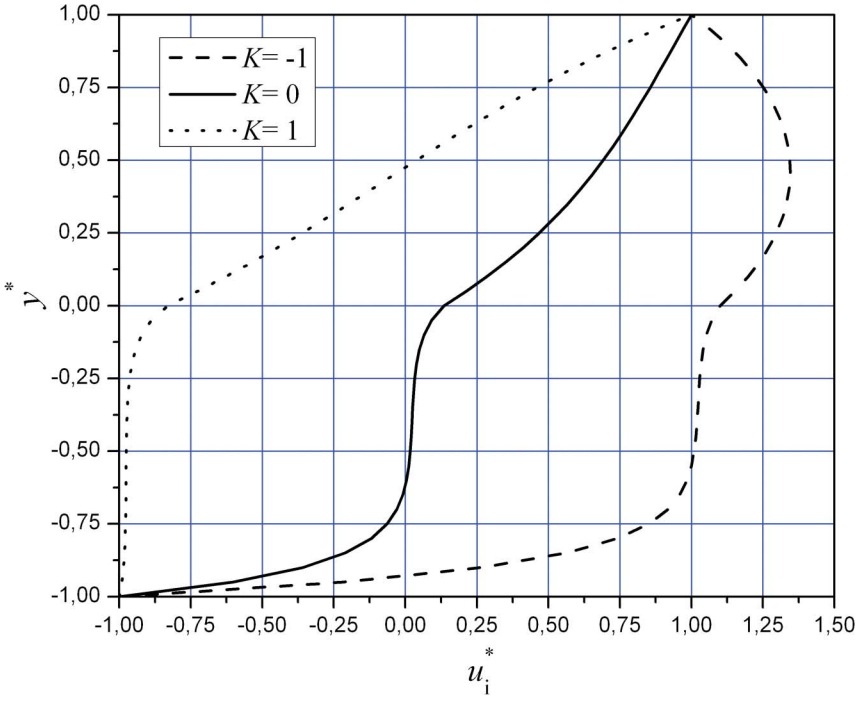

Fig. 8. Temperature profiles for different values of load factor ($Ha_1 = 2$; $Ha_2 = 10$; $\lambda = 1$; $\alpha = 0.66$; $\gamma = 0.025$; $\xi = 0.06$).

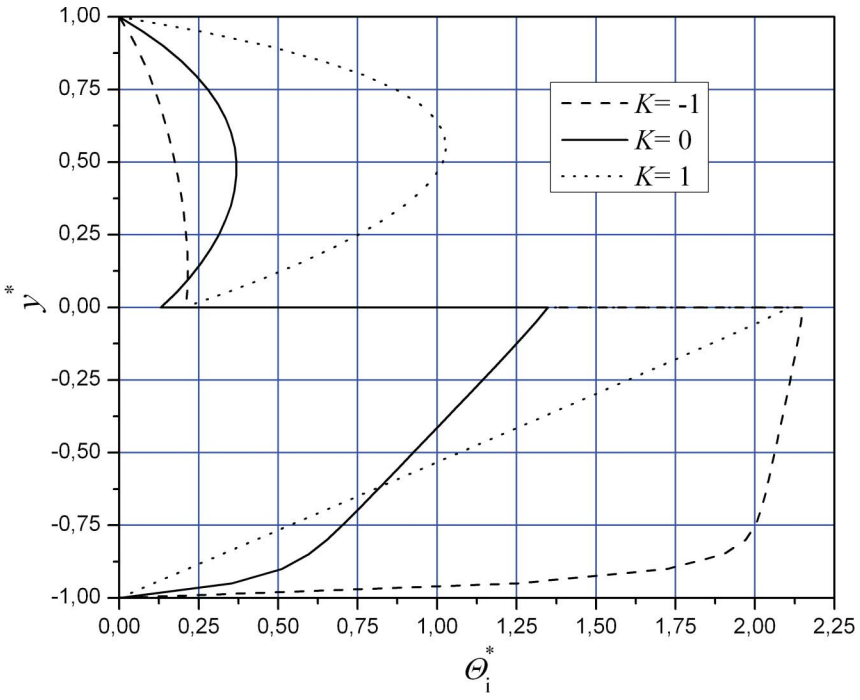

Fig. 9. Velocity profiles for different values of load factor ($Ha_1 = 2$; $Ha_2 = 10$; $\lambda = 1$; $\alpha = 0.66$; $\gamma = 0.025$; $\xi = 0.06$).

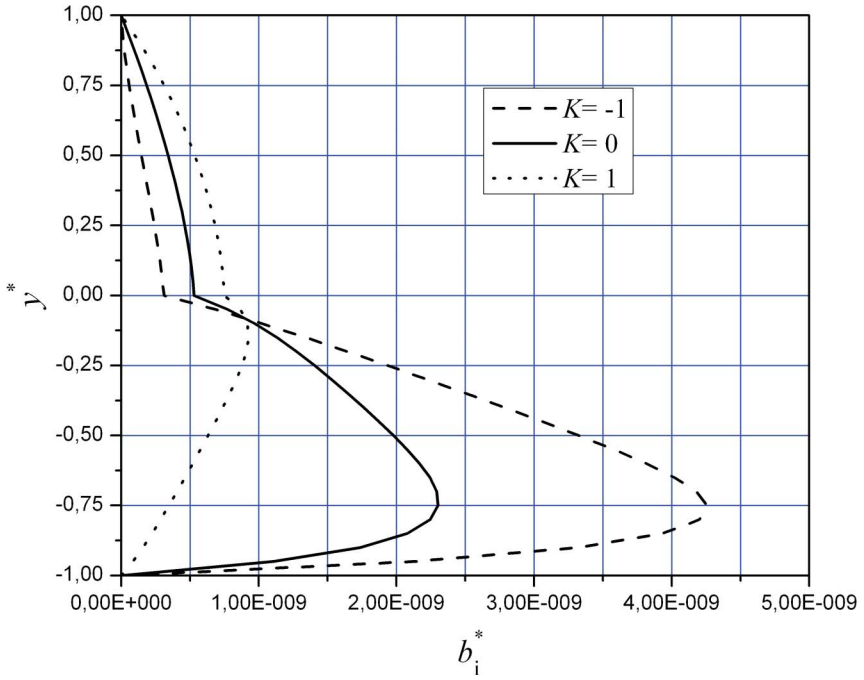

Fig. 10. Ratio of an induced and applied magnetic field for different values of load factor ($Ha_1 = 2$; $Ha_2 = 10$; $\lambda = 1$; $\alpha = 0.66$; $\gamma = 0.025$; $\xi = 0.06$).

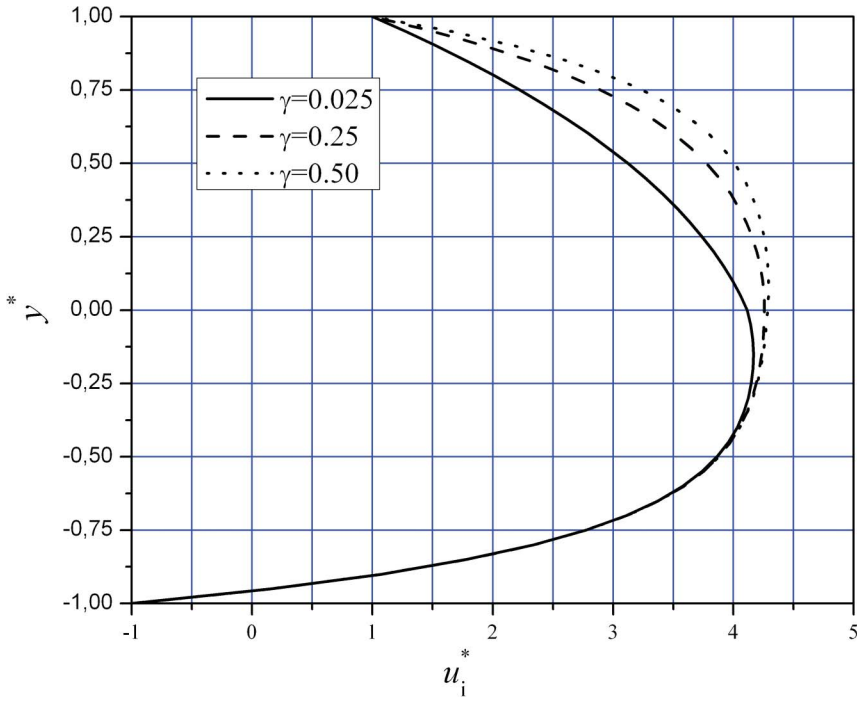

Fig. 11. Velocity profiles for different values of electrical conductivities ratio γ ($K = -2$; $\lambda = 1$; $\alpha = 0.66$; $\xi = 0.06$).

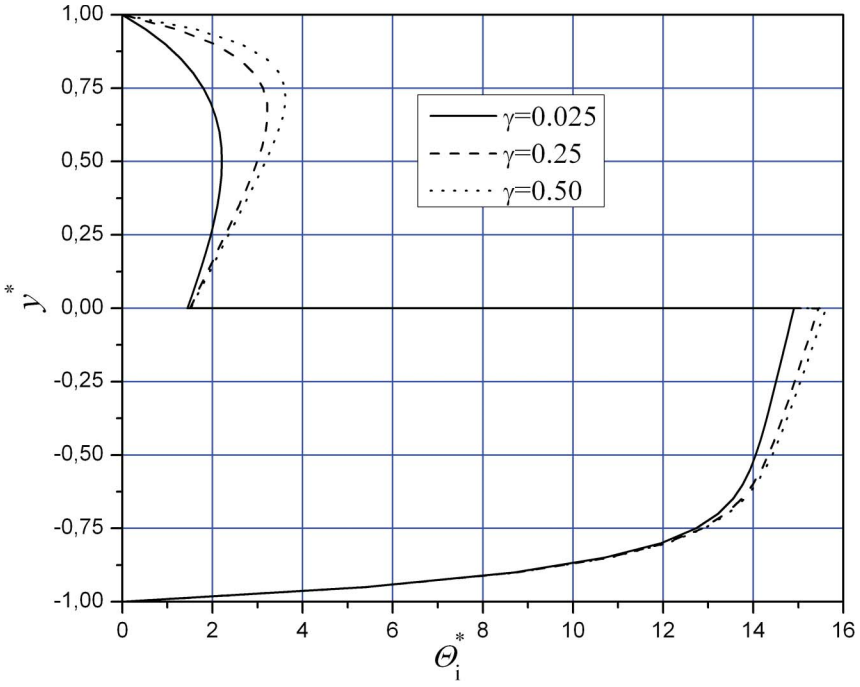

Fig. 12. Temperature profiles for different values of electrical conductivities ratio γ ($K=-2$; $\lambda=1$; $\alpha=0.66$; $\xi=0.06$).

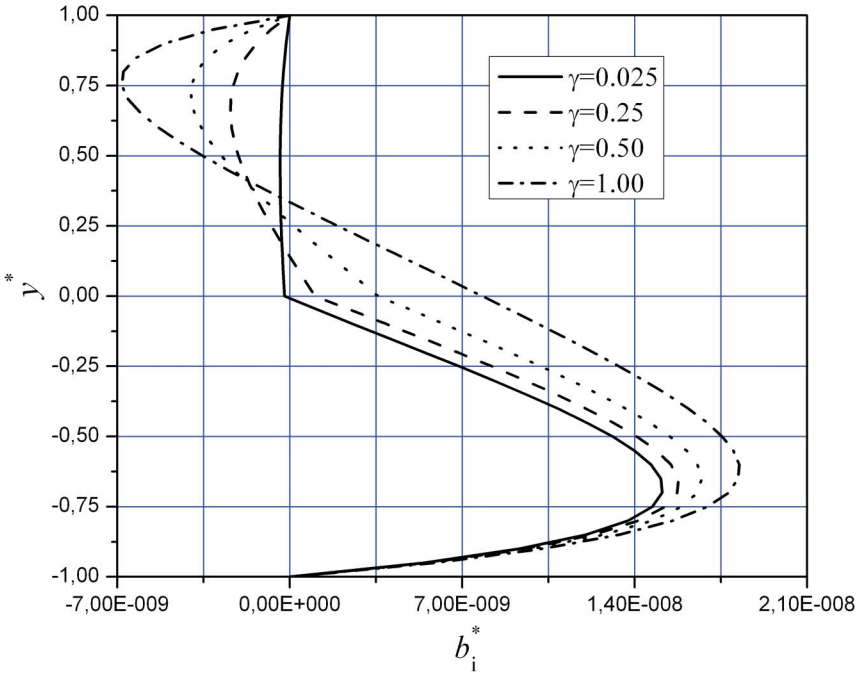

Fig. 13. Ratio of an induced and applied magnetic field for different values of electrical conductivities ratio γ ($K=-2$; $\lambda=1$; $\alpha=0.66$; $\xi=0.06$).

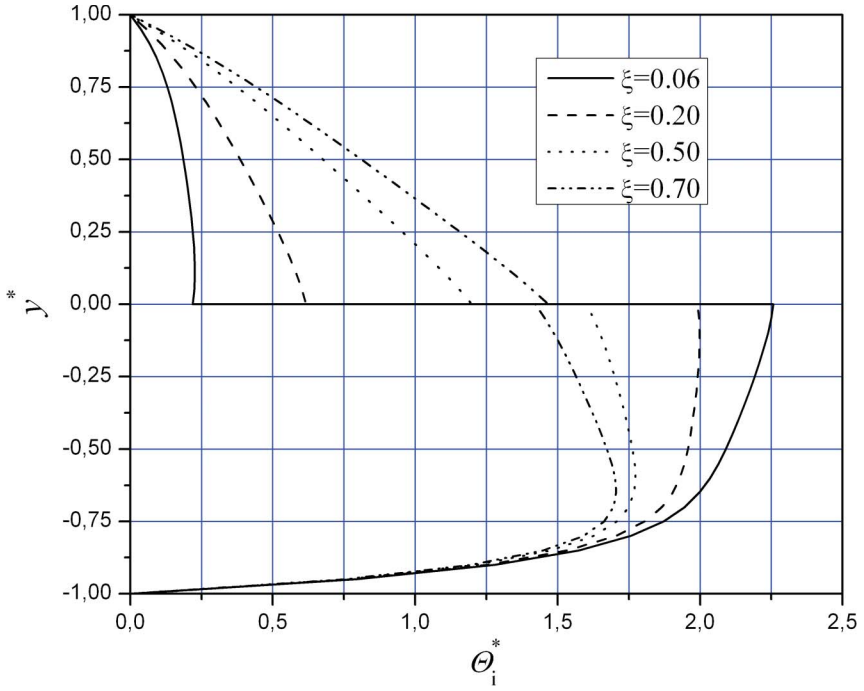

Fig. 14. Temperature profiles for different values of ratio of thermal conductivities ξ ($Ha_1 = 2$; $Ha_2 = 10$; $K = -1$; $\lambda = 1$; $\alpha = 0.66$; $\gamma = 0.025$).

temperature is continuous across the interface). This choice was made because of mathematical simplification and its direct consequence is the difference (temperature jump) that occurs at the interface. This difference is directly proportional to the thermal conductivities ratio of fluids ξ, and inversely proportional to the ratio of viscosities α, while the S^* is zero when the temperatures of the upper and lower plate are equal ($\Theta_1(0) = (\xi/\alpha)\Theta_2(0) + S^*$).

It can be seen from Figs. 2 and 3 that the magnetic field flattens out the velocity and temperature profiles and reduces the flow energy transformation as the inclination angle decreases. The ratio of an induced and externally imposed magnetic field, for the $K = 0$ (short-circuit condition) and various values of magnetic field inclination, is shown in the Fig. 4. Disturbance of the external magnetic field is directly proportional to the magnetic Reynolds number and essentially depends on the regime of the channel load and inclination of the applied magnetic field. In the observed case the magnetic Reynolds numbers are small ($Rm_1 \sim 10^{-9}$,$Rm_2 \sim 10^{-7}$) and hence the induced field is small, but the general conclusions represented in the paper are valid also for higher values.

Figure 4 shows increase in the ratio of magnetic fields as the inclination angle of an applied field decreases. In observed case for the bottom half of the channel this ratio have tendency to move the maximum value closer to the lower plate while λ increase.

Figures 5 to 7 depict the effect of the Hartmann number on velocity, temperature and induced magnetic field, while the electrical load factor K is equal to zero (so-called short-circuit condition).

In the Fig. 5 are shown the velocity profiles over the channel height for several values of the Hartmann number. It can clearly be seen that as the Hartmann number is increased, the velocity profiles become flatter, and velocity gradient near the plates become steeper. In other words, the force necessary to move these plates is greater, the larger Ha. The influence of the Hartmann

number on the velocity field was more pronounced in the channel region 2 containing the fluid with greater electrical conductivity. It was found that for larger values of the Hartmann number flow can be almost completely stopped in the region 2, while the velocity decrease is significant in region 1.

The Fig. 6 shows the influence of the Hartmann number on the dimensionless temperature. Several interesting observations can readily be made. First, it should be recalled that, in the solution, both viscous heating and Joule heating were included in the analysis. As expected, the stronger the magnetic field, the more the flow is retarded in the middle of the channel. As the plates move, viscous heating are more pronounced in areas close to them. With the increase of the Hartmann number temperature in the middle of the channel decreases, which corresponds to the results presented by Smolentsev et al. [27], while near the plate's increases due to viscous heating resulted from large shear stresses and Joule heating.

In general, the effect of increasing the Hartmann number on temperature profiles in both of the parallel-plate channel regions was in equalizing the fluid temperatures.

Effect of increasing the Hartman number on the ratio of induced and applied magnetic field in the middle of the channel is similar to the influence on temperature, as can be seen from the Fig. 7. This ratio decreases with increase of the Hartmann number. Ratio of an induced and applied magnetic field is more pronounced in the channel region 2 containing more conductive fluid. The influence of the induced magnetic field for chosen fluid pair in the considered case is not so pronounced, but in case of higher values of the magnetic Reynolds number, the knowledge of the applied and induced field ratio have great significance. It is characteristic that the induced magnetic field leads to the occurrence of transverse pressure gradient, without changing the hydrodynamics of flow. Increase of the transverse pressure gradient may lead to flow instability at the interface of two fluids.

Of particular significance is the analysis when the load factor K is different from zero (value of load factor K define the system as generator, flow-meter or pump).

In the Fig. 8 the temperature distribution as a function of y^*, for various values of K, is shown. When $K=0$, the channel is short-circuited and all current flows in one direction. In this case the temperature distribution is affected by the viscous dissipation and Joule heating. For the lower fluid viscosity dissipation is expressed close to the plate, and towards the middle of the channel temperature distribution is dominated by Joule heating. When the channel operates in the open-circuit condition, and $K=-1$, the current flow is so small that viscous dissipation dominates the temperature distribution. Temperature rise is particularly pronounced at the lower fluid. On account of this increase, the temperature of the upper fluid also increases in the middle of the channel. Due to the absence of Joule heating fluid in the region 1 now has a smaller temperature in the upper zone compared to the previous case ($K=0$). Now when $K=1$, the current flow is quite large, and since the Joule heating depends on the square of the current, temperature increases throughout the channel compared to the short-circuit condition. In this case lower fluid is affected only by the Joule heating, while the fluid in region 1 is affected by both heating effects.

Figure 9 shows the effect of the load factor on the velocity distribution. As can be seen, for a fixed Hartman number, a $K=1$ will decrease the pressure gradient while a $K=-1$ will increase it. The results show the ability to change the direction of flow, although the plates move in a certain direction. Also, significant increase in the flow is achieved for negative values of K.

The obtained results show that different values of the inclination angle, the Hartmann number and the load factor is a convenient control method for heat and mass transfer processes.

Figure 10 shows the change of induced field, over the channel height, for different values of the load factor. The curve for $K=0$ correspond to the already discussed case. The curves for $K\neq 0$ shows the fact that the induced field directly related to the total current in the channel and velocity. With the change of the parameter K curves of the magnetic induction lies in the other direction, as a result of the current flowing in the opposite direction. The ratio of an induced and applied magnetic field has a considerable change when the load parameter is different from zero, especially in region 2.

As for certain fluids used in technical practice is very easy to change the electrical conductivity without significant changes in other physical properties, it is interesting to consider the influence of electrical conductivities ratio γ on the temperature, velocity and induced magnetic field.

The effect of the ratio of electrical conductivities of the fluids in regions 1 and 2 on the velocity profiles is shown in Fig. 11. The presented results refer to the case when the load factor is equal to -2. When $K=-2$, all the current flows to the right in the channel, and it must be presumed that this net current flow has been supplied by an external power supply. This is the case of an MHD accelerator or pump. It can clearly be seen that as the ratio of electrical conductivities is increased, the velocity profile for the fluid in region 1 becomes flatter, and the velocity gradient near the upper plate becomes steeper. As the electrical conductivity of the lower fluid does not change, change of velocity in Region 2 is expressed only at the interface and this is a consequence of the mutual effects of fluids.

In the Fig. 12 the temperature distribution as a function of y^*, for various values of γ, is shown. The effect of ratio of the electrical conductivities of the two fluids on temperature field is quite similar compared with the effect on velocity field, which is evident from this Figure. It is found that the effect of increasing γ is to increase the temperature field in the region 1. In this case, viscous dissipation for both fluids was expressed near the plates, while the Joule heating is dominant in the middle of the channel. Temperature rise in the middle of the channel is a consequence of Joule heat, which increases with the increase of electrical conductivity of the upper fluid. Although the effect of viscous dissipation is now smaller in the middle of the channel, the total temperature increases due to mutual effects of fluids at the interface.

The effect of the ratio of electrical conductivities of the fluids on the induced magnetic field is shown in Fig. 13. It is interesting to note that the increase of the parameter γ changes significantly the ratio of induced and applied magnetic field in region 1, while this ratio changes very slowly in Region 2. In the case when the parameter γ equal to 1, i.e. when the electrical conductivities of the fluids are the same, profile of induced field becomes very similar to Hartmann flow. The difference in relation to the Hartmann flow is reflected in the incomplete symmetry around the axis of the channel as a result of plate's movement.

Figure 14 shows the temperature distribution over the channel height for different values of the fluids thermal conductivities ratio ξ. Increases in the thermal conductivity ratio have the tendency to cool down the thermal state in the channel region 2, and to decrease the heat flux at the interface. This is depicted in the equalizing of the temperature field as ξ increases as shown in Fig. 14.

6 CONCLUSIONS

The problem of MHD flow and heat transfer of two immiscible fluids between horizontal moving parallel plates in the presence of applied electric and inclined magnetic field was investigated analytically. Separate closed form solutions for velocity, temperature and magnetic induction of each fluid were obtained, numerically evaluated and presented graphically for two fluids important for technical practice.

Numerical results for the effects of the applied magnetic field inclination angle, Hartmann number, load factor and ratio of fluid electrical and thermal conductivities on the discussed MHD flow have shown:

- Decrease of applied magnetic filed inclination angle increase the ratio of induced and applied magnetic field and flattens out the velocity and temperature profiles.
- With the increase of the Hartmann number temperature in the middle of the channel decreases, velocity profiles become flatter, and velocity gradient near the plates become steeper. Near the plate's temperature increases due to viscous heating resulted from large shear stresses and Joule heating.
- Magnetic induction is evidently suppressed with an increase in the applied magnetic field.
- For a fixed Hartman number, positive values of load factor will decrease the pressure gradient while negative will increase it.
- When the channel operates in the open-circuit condition viscous dissipation dominates the temperature distribution. When current flow has been supplied by an external power supply temperature increases throughout the channel due to the Joule heating.
- With the change of the load factor curves of the magnetic induction reverse lines direction, as a result of the current flowing in the opposite direction.
- Increase of the electrical conductivities ratio changes significantly the ratio of induced and applied magnetic field in region 1 and profile of induced field becomes very similar to the Hartmann flow.
- Increases in the thermal conductivities ratio have the tendency to cool down the thermal state in the channel region 2, and to decrease the heat flux at the interface.

Acknowledgements

The authors are grateful to the reviewers for their useful comments and suggestions.

REFERENCES

1. Blum, E.L., Zaks, M.V., Ivanov, U.I. and Mikhailov, Yu.A., *Heat and Mass transfer in the Presence of an Electromagnetic Field*, (in Russian), Zinatne, Riga, 1967,
2. Hunt, J. C. R. and Holroyd, R.J., "Applications of laboratory and theoretical MHD duct flow studies in fusion reactor technology," *Technical Report CLM-R169, Culham Laboratory*, 1977.
3. Morley, N.B., Malang, S. and Kirillov, I., "Thermo-fluid magnetohydrodynamic issues for liquid breeders," *Fusion Science and Technology*, Vol. 47, pp. 488–501, 2005.
4. Davidson, P.A., "Pressure forces in the MHD propulsion of submersibles," (in Russian), *Magnetohydrodynamics*, Vol. 29, No. 3, pp. 49–58, 1993.
5. Tsinober, A., "MHD-drag reduction, in: viscous drag reduction in boundary layers," *AIAA Progress in Aeronautics and Astronautics,* Vol. 123, eds. Bushnell, D.M. and Hefner, J.N., pp. 327–349, 1990.
6. Boričić, Z., Nikodijević, D., Obrović, B. and Stamenković, Ž., "Universal equations of unsteady two-dimensional MHD boundary layer whose temperature varies with time," *Theoretical and Applied Mechanics,* Vol. 36, No. 2, pp. 119–135, 2009.
7. Obrović, B., Nikodijević, D. and Savić, S., "Boundary layer of dissociated gas on bodies of revolution of a porous contour," *Strojniški vestnik - Journal of Mechanical Engineering*, Vol. 55, No. 4, pp. 244–253, 2009.

8. Xu, H., Liao, S.J. and Pop, I., "Series solutions of unsteady three-dimensional MHD flow and heat transfer in the boundary layer over an impulsively stretching plate," *European Journal of Mechanics B/Fluids*, Vol. 26, pp. 15–27, 2007.
9. Nikodijević, D., Boričić, Z., Blagojević, B. and Stamenkovic, Ž., "Universal solutions of unsteady two-dimensional MHD boundary layer on the body with temperature gradient along surface," *WSEAS Transactions on Fluid Mechanics*, Vol. 4, No. 3, pp. 97–106, 2009.
10. Kessel, C.E., Meade, D. and Jardin, S.C., "Physics basis and simulation of burning plasma physics for the fusion ignition research experiment (FIRE)," *Fusion Engineering and Design*, Vol. 63–64, pp. 559–567, 2002.
11. Tzirtzilakis, E.E., "A mathematical model for blood flow in magnetic field," *Physics of Fluids*, Vol. 17, Issue 7, pp. 077103/1–077103/15, 2005,
12. Bird, R.B., Stewart, W.E. and Lightfoot, E.N., "*Transport phenomena*," Wiley, New York, 1960.
13. Bhattacharya, R.N., "The flow of immiscible fluids between rigid plates with a time dependent pressure gradient," *Bulletin of the Calcutta Mathematical Society*, Vol. 1, pp. 129–137, 1968.
14. Mitra, P., "Unsteady flow of two electrically conducting fluids between two rigid parallel plates," *Bulletin of the Calcutta Mathematical Society*, Vol. 74, pp. 87–95, 1982.
15. Chamkha, A.J., "Flow of two-immiscible fluids in porous and non-porous channels," *ASME Journal of Fluids Engineering*, Vol. 122, pp. 117–124, 2000.
16. Alireza, S. and Sahai, V., "Heat transfer in developing magnetohydrodynamic poiseuille flow and variable transport properties," *International Journal of Heat and Mass Transfer*, Vol. 33, No. 8, pp. 1711–1720, 1990.
17. Malashetty, M.S. and Leela, V., "Magnetohydrodynamic heat transfer in two fluid flow," *Proceeding of national heat transfer conference on AIChE and ASME HTD*, pp. 159–167, 1991.
18. Malashetty, M.S. and Leela, V., "Magnetohydrodynamic heat transfer in two phase flow," *International Journal of Engineering Sciences*, Vol. 30, pp. 371–377, 1992.
19. Packham, B.A., Shail, R., "Stratified laminar flow of two immiscible fluids," *Proceedings Cambridge Philosophical Society*, Vol. 69, pp. 443–448, 1971.
20. Lohrasbi, J., Sahai, V., "Magnetohydrodynamic heat transfer in two phase flow between parallel plates," *Applied Scientific Research*, Vol. 45, pp. 53–66, 1988.
21. Malashetty, M.S., Umavathi, J.C. and Kumar, J.P., "Convective MHD two fluid flow and heat transfer in an inclined channel," *Heat and Mass Transfer*, Vol. 37, pp. 259–264, 2001.
22. Malashetty, M.S., Umavathi, J.C. and Kumar, J.P., "Two fluid flow and heat transfer in an inclined channel containing porous and fluid layer," *Heat and Mass Transfer*, Vol. 40, pp. 871–876, 2004.
23. Umavathi, J.C., Mateen, A., Chamkha, A.J. and Mudhaf, A.A., "Oscillatory hartmann two-fluid flow and heat transfer in a horizontal channel," *International Journal of Applied Mechanics and Engineering*, Vol. 11, No. 1, pp. 155–178, 2006.
24. Umavathi, J.C., Mateen, A., Chamkha, A.J. and Mudhaf, A.A., "Unsteady two-fluid flow and heat transfer in a horizontal channel," *Heat Mass Transfer*, Vol. 42, pp. 81–90, 2005
25. Malashetty, M.S., Umavathi, J.C. and Kumar, J.P., "Magnetoconvection of two immiscible fluids in vertical enclosure," *Heat and Mass Transfer*, Vol. 42, pp. 977–993, 2006.
26. Misuri, T. and Andrenucci, M., "Tikhonov's MHD channel theory: a review," *30th International Electric Propulsion Conference*, Florence, Italy, September 17–20, 2007.
27. Smolentsev, S. Yu., Tananaev, A.V., Dajeh, D.A. and Shmarov, V.S., "Laminar heat transfer in MHD-flow in a rectangular duct. 2. Experimental studies," *Magnetohydrodynamics*, Vol. 33, No. 2, pp. 155–160, 1997.